



**HAL**  
open science

## **Geological evolution of Ares Vallis on Mars: Formation by multiple events of catastrophic flooding, glacial and periglacial processes**

Andrea Pacifici, Goro Komatsu, Monica Pondrelli

### ► **To cite this version:**

Andrea Pacifici, Goro Komatsu, Monica Pondrelli. Geological evolution of Ares Vallis on Mars: Formation by multiple events of catastrophic flooding, glacial and periglacial processes. *Icarus*, 2009, 202 (1), pp.60. <10.1016/j.icarus.2009.02.029>. <hal-00545289>

**HAL Id: hal-00545289**

**<https://hal.science/hal-00545289v1>**

Submitted on 10 Dec 2010

**HAL** is a multi-disciplinary open access archive for the deposit and dissemination of scientific research documents, whether they are published or not. The documents may come from teaching and research institutions in France or abroad, or from public or private research centers.

L'archive ouverte pluridisciplinaire **HAL**, est destinée au dépôt et à la diffusion de documents scientifiques de niveau recherche, publiés ou non, émanant des établissements d'enseignement et de recherche français ou étrangers, des laboratoires publics ou privés.



HAL Authorization

## Accepted Manuscript

Geological evolution of Ares Vallis on Mars: Formation by multiple events of catastrophic flooding, glacial and periglacial processes

Andrea Pacifici, Goro Komatsu, Monica Pondrelli

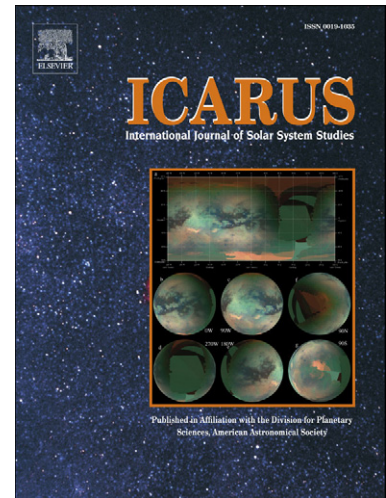
PII: S0019-1035(09)00109-2  
DOI: [10.1016/j.icarus.2009.02.029](https://doi.org/10.1016/j.icarus.2009.02.029)  
Reference: YICAR 8953

To appear in: *Icarus*

Received date: 26 March 2008  
Revised date: 16 January 2009  
Accepted date: 27 February 2009

Please cite this article as: A. Pacifici, G. Komatsu, M. Pondrelli, Geological evolution of Ares Vallis on Mars: Formation by multiple events of catastrophic flooding, glacial and periglacial processes, *Icarus* (2009), doi: [10.1016/j.icarus.2009.02.029](https://doi.org/10.1016/j.icarus.2009.02.029)

This is a PDF file of an unedited manuscript that has been accepted for publication. As a service to our customers we are providing this early version of the manuscript. The manuscript will undergo copyediting, typesetting, and review of the resulting proof before it is published in its final form. Please note that during the production process errors may be discovered which could affect the content, and all legal disclaimers that apply to the journal pertain.



1 **Geological evolution of Ares Vallis on Mars: Formation by multiple events of catastrophic flooding,**  
2 **glacial and periglacial processes**

3  
4 Andrea Pacifici, Goro Komatsu, Monica Pondrelli

5  
6 International Research School of Planetary Sciences

7 Dipartimento di Scienze

8 Università d'Annunzio

9 Viale Pindaro, 42

10 65127 Pescara

11 Italy

12  
13 Email addresses:

14  
15 A. Pacifici: [pacifici@irsps.unich.it](mailto:pacifici@irsps.unich.it)

16 G. Komatsu: [goro@irsps.unich.it](mailto:goro@irsps.unich.it)

17 M. Pondrelli: [monica@irsps.unich.it](mailto:monica@irsps.unich.it)

18  
19  
20  
21  
22 Manuscript:

23 Pages: 50

24 Figures: 20

25 Tables: 0

26  
27  
28  
29 Running head:

30

31

**Geological evolution of Ares Vallis, Mars.**

32

33

34

Corresponding author:

35

36

Andrea Pacifici

37

International Research School of Planetary Sciences

38

Dipartimento di Scienze

39

Università d'Annunzio

40

Viale Pindaro, 42

41

65127 Pescara

42

Italy

43

44

45

46

47

48

49

50

51

52

53

54

55

56

57

58

59        **Abstract**

60        Ares Vallis is one of the greatest outflow channels of Mars. Using high-resolution images of recent  
61 missions to Mars (MGS, 2001 Odyssey, and Mars Express), we investigated Ares Vallis and its valley arms,  
62 taking advantage of 3-dimensional analysis performed using the high-resolution stereo capability of the Mars  
63 Express High Resolution Stereo Camera (HRSC). In our view, Ares Vallis is characterized by catastrophic  
64 flood landscapes partially superimposed by ice-related morphologies. Catastrophic flood landforms include  
65 erosional terraces, grooved terrains, streamlined uplands, giant bars, pendant bars, and cataract-like features.  
66 Ice-related morphologies include probable kame features, thermokarstic depressions, and patterned grounds.  
67 Our investigations outline that throughout the Hesperian age, Ares Vallis and its valley arms had been  
68 sculpted by several, time-scattered, catastrophic floods, originating from Iani, Hydaspis and Aram Chaos.  
69 Geomorphological evidence suggests that catastrophic floods were ice-covered, and that climatic conditions  
70 of Mars at this time were similar to those of the present day. At the end of each catastrophic flood, ice  
71 masses grounded, forming a thick stagnant dead-ice body. Each catastrophic flood was followed by a  
72 relatively brief period of warmer-wetter climatic conditions, originated as a consequence of catastrophic  
73 flooding. During such periods thermokarstic depressions originated, liquid water formed meandering  
74 channels, and ice-contact deposits were emplaced by ice-walled streams. Finally, the climate turned into  
75 cold-dry conditions similar to the present-day ones, and ice masses sublimated.

76

77

78        **Keywords:** Mars, surface; Mars, climate; Geological processes; Ices.

79

80

81

82        **1 - Introduction**

83        Outflow channels on Mars are large complexes of fluid-eroded troughs up to 100 km wide and 2000  
84 km long. The flows that formed Martian outflow channels appear to have emanated from discrete collapse  
85 zones or chaotic terrains (Baker, 1982). Ares Vallis (fig. 1) is one of the greatest among these: it is a trough  
86 1500 km long originating from Iani Chaos, etching Noachian and Early Hesperian cratered plateaus, and  
87 debouching in Chryse Planitia.

88 Ares Vallis has been deeply investigated in the past decades, partially to support landing site  
89 analyses of the NASA Pathfinder, which landed near the present termination of Ares Vallis on July 4, 1997.  
90 Several geologic interpretations of Ares Vallis have been proposed. Baker and Milton (1974), Baker (1982),  
91 Baker et al. (1992), Komatsu and Baker (1997) hypothesize that Ares Vallis was carved by catastrophic  
92 floods. Glicken and Schultz (1980) propose that Ares Vallis originated by giant clay-rich volcanic mud  
93 flows. Lucchitta et al. (1981) and Lucchitta (1982, 2001) suggest ice-sculpturing processes. Costard (1989)  
94 proposes a fluvio-thermal erosion. Robinson et al. (1996) consider that it was formed by glacial processes  
95 with some fluvial activity. Marchenko et al. (1998) investigated the mouth of Ares Vallis and interpreted it as  
96 shaped by multiple catastrophic flood events. Nelson and Greeley (1999) suggest an initial sheetwash  
97 followed by deepening of channels caused by subsequent floodings. Tanaka (1999) propose catastrophic  
98 outbreak of water from pressurized aquifers, evolving into debris flows. Furthermore, thermokarstic  
99 landforms and processes along Ares Vallis have been reported by some works (Costard and Dollfus, 1986;  
100 Costard and Kargel, 1995; Costard and Baker, 2001). Leverington (2004) proposes a volcanic origin. The  
101 hypotheses regarding the origin of Martian outflow channels are summarized in Baker et al. (1992) and Carr  
102 (1996). Each model of origin and evolution implies different processes of the Ares Vallis formation and  
103 different climatic evolutions of Mars. Almost all the proposed models derive from observations carried out  
104 using mainly Mariner and Viking data with low-medium spatial resolutions (some tens to few hundreds of  
105 meters for each pixel). Aims of this work, therefore, are: i) to investigate Ares Vallis with high-resolution  
106 images (HRSC, THEMIS VIS and MOC narrow angle), ii) to describe new observed morphologies, and  
107 according to these, iii) to hypothesize new possible scenarios illustrating the geologic history of Ares Vallis.  
108 Our observations are based mainly on a detailed geomorphological map of Ares Vallis recently published by  
109 Pacifici (2008).

110

111

## 112 2 – Datasets

113 The High Resolution Stereo Camera (HRSC), on board the ESA mission Mars Express, provides  
114 orthorectified images and stereo-derived Digital Terrain Models (DTMs). The orthorectified images are  
115 provided both in gray scale (obtained by nadir channel) and in color (with pan-sharpening of nadir channel).  
116 HRSC images fill the gap in cell size between high-resolution small-footprint images (e.g., MGS MOC

117 narrow angle) and low-resolution large-footprint images (e.g., Viking, Mars Global Surveyor MOC wide  
118 angle and Mars Odyssey THEMIS infra-red), over very large areas. Such characteristics of the HRSC images  
119 are very helpful in order to observe stratigraphic correlations and wide-ranging, small-scale morphologies.  
120 Furthermore, HRSC data allow draping of high-resolution images on stereo-derived DTMs, and their  
121 observation in 3-dimensional view.

122 Twenty-one HRSC orbit datasets covering entire Ares Vallis were processed in order to provide  
123 images with resolutions between 12.5 and 50 m/pixel, and derived DTMs with a spatial resolution of about  
124 200 m/pixel. We complemented the HRSC datasets with other mission datasets such as Viking, Mars Global  
125 Surveyor MOC wide angle (MOC WA), and Mars Odyssey THEMIS (both Visible and IR). MOC narrow  
126 angle (MOC NA) images were used to further characterize the observed morphologies with much more  
127 details. The Mars Odyssey THEMIS infra-red (THEMIS IR) data were used in order to characterize also  
128 thermal properties of surfaces. Regarding thermal properties, we performed only qualitative and not  
129 quantitative observations in this work. Finally, Mars Global Surveyor MOLA-megdr grid data were used to  
130 conduct regional topographic analysis.

131

### 132 **3 – Physiographic and geological setting of Ares Vallis**

133 Two main reaches characterize Ares Vallis. The upper reach (Narrow Ares Vallis) is about 25 km  
134 wide and 1500 m deep. A few erosional terraces characterize its steep walls and broad, shallow, and  
135 anastomosing channels occur on the surrounding plateaus. The lower reach (Wide Ares Vallis) is about 100  
136 km wide, and it is shallower and wider and its walls are less steep approaching the valley termination.  
137 Widths of both the reaches are generally constant and the transition between them is evident.

138 Three valley arms tens of kilometers wide merge with Ares Vallis. We appoint these valleys with the  
139 informal names of Eastern Valley, Western Valley, and Aram Chaos Channel (fig. 1). Eastern Valley is a  
140 trough about 20 km wide and 1 km deep, hanging above Ares Vallis. Similar to Ares Vallis, Eastern Valley  
141 originates from Iani Chaos but at a more marginal (eastern) position and higher altitudes. The valley merges  
142 into the upper reach of Ares Vallis with a hanging morphology and a difference in altitude of about 600 m.  
143 Western Valley is a broad and shallow trough emanating from Hydaspis Chaos and hanging above Ares  
144 Vallis. It extends for about 370 km, varies in width from 40 km to 160 km, and terminates with a hanging  
145 morphology with a difference in altitude of about 900 m. Western Valley shows gently-sloping walls and lies

146 about 1000 m below the neighboring plateaus. Aram Chaos Channel is a narrow and deep trough emanating  
147 from Aram Chaos and merging with Ares Vallis. Using the term ‘the Ares Vallis Complex’ we will refer to  
148 Ares Vallis and its incoming troughs.

149 A longitudinal topographic profile of the Ares Vallis floor (fig. 2) shows that the narrower upper  
150 reach of Narrow Ares Vallis has a steeper topographic gradient on average. The deepest point of Iani Chaos,  
151 which is believed to be one of the main source areas for fluids eroding Ares Vallis (Komatsu and Baker,  
152 1997), lies about 800 m below the beginning of Narrow Ares Vallis. Floors of Wide Ares Vallis lie about  
153 200 m above the lowest floors of Narrow Ares Vallis, and its topographic profile appears to be irregular at  
154 the upstream portion and flat on the downstream portion. The present-day termination of Ares Vallis consists  
155 of a scarp 50–200 m high, which was formed by Tiu-Simud Valles flows postdating Ares Vallis (Marchenko  
156 et al., 1998; Nelson and Greeley, 1999; Costard and Baker, 2001).

157 Regarding ages of Ares Vallis surfaces, Tanaka et al. (2005) map five units in the area. They vary in  
158 ages from Middle Noachian to Late Hesperian. Hartmann (2005) also indicates a Late Hesperian age for the  
159 Ares Vallis floor and its surroundings. Pacifici (2008) suggests ages varying from Early to Late Hesperian.  
160 Werner (2005) observes that ages of the northern reach of Iani Chaos vary from 3.5 Ga to 50 Ma, while the  
161 upper reach of Ares Vallis shows ages varying from 650 to 40 Ma.

162

#### 163 **4 - Geomorphological analysis**

164 We observe in the Ares Vallis Complex two different typologies of geomorphological features. The  
165 first one includes grooved terrains, streamlined uplands, giant bars, pendant bars, cataract-like features and  
166 hanging valleys, resembling terrestrial morphologies that are believed to have been shaped by catastrophic  
167 floods. The second typology includes ice-contact features, thermokarstic depressions, and patterned grounds.  
168 These ice-related features overlap and postdate catastrophic flood morphologies. All these features are  
169 described below in detail.

170

#### 171 **4.1. Catastrophic flood features**

##### 172 *4.1.1. Erosional terraces and hanging valleys*

173 Along the upper reach of Ares Vallis, there are terraces (fig. 3) occurring (at least) at five different  
174 altitude levels. Each terrace seems to have been sculpted by one (or more) catastrophic flooding, originated

175 by an enormous release of water emanating from chaotic terrains. A terrace occurring at the highest altitude  
176 consists of a very large area extending mainly northeast of Narrow Ares Vallis. This terrace is delineated by  
177 the -2000 m contour line, and it is characterized by a smooth-texture on medium-resolution images (15-50  
178 m/pixel). Locally, shallow anastomosing channels occur. This terrace corresponds to the areas produced by  
179 the first floods emanating from Iani Chaos. Terraces occurring at lower altitudes mark subsequent floods and  
180 illustrate progressive deepening and channelization of Ares Vallis. They develop laterally to the entire widths  
181 of Ares Vallis and often show a grooved surface. The grooved surface of the terraces suggests that it was  
182 sculpted mainly by erosive processes.

183 Eastern and Western Valley arms are truncated by the Ares Vallis main channel and hang over its  
184 floors. Crosscutting relationships among Eastern Valley and the erosional terraces of Ares Vallis show that  
185 Eastern Valley originated during the first four catastrophic flood events (fig. 3), and then became abandoned  
186 during the subsequent events.

187 Western Valley (fig. 4) is a broad and shallow trough characterized by the absence of erosional  
188 terraces. This suggests that Western Valley was formed during one single catastrophic flood emanating from  
189 Hydaspis Chaos. If multiple floods indeed occurred, they did not leave any observational evidence.  
190 Crosscutting relationships between Western Valley and Ares Vallis suggest that such catastrophic flood  
191 event occurred between the second and fourth catastrophic flood events of Ares Vallis.

192 Aram Chaos Channel is a deep and narrow gorge in which erosional terraces are consequently  
193 poorly extended. On the base of high-resolution images we hypothesize that Aram Chaos Channel was  
194 carved by at least two catastrophic floods (possibly more), which occurred at the same time of last floods  
195 emanating from Iani Chaos.

196

197

#### 198 *4.1.2. Grooved terrains*

199 Grooved terrains characterize a large part of Ares Vallis Complex. They occur mainly on top of  
200 erosional terraces, and on the valley floors as patches. Grooved terrains occur both at the proximal and at the  
201 distal portions of Ares Vallis troughs. Grooves appear to consist of equally-spacing furrows or trenches  
202 between narrow ridges (fig. 5a and 5c) that extend along the direction of the flow. They are hundreds of  
203 meters wide, hundreds of meters spaced, and about a few to tens of kilometers long. Groove depths are not

204 estimated due to their small scales. The overall morphology of such features resembles those of some  
205 terrestrial mega-flutes (fig. 5d and 5e). On the base of relationships among grooves and neighboring  
206 morphologies it is possible to assess certain morphological and geological properties of the grooved terrains.  
207 The grooved terrains appear to be locally etched and postdated by narrow, meandering channels (fig. 6),  
208 which typically emanate from flat-floored impact craters or from shallow, flat-floored irregularly-shaped  
209 depressions. Comparison between channels and grooves, and their geometrical relationships, allows  
210 hypothesizing that grooves are no more than meters or a few tens of meters deep. In areas where water  
211 flowed deeper and longer (i.e. on the main stream of Ares Vallis) grooves appear wider and deeper than in  
212 areas where water flowed shallower and for shorter time (i.e. Western Valley). Moreover, relationships  
213 among meandering channels and grooves seem to indicate that grooved terrains consist of relatively “soft”  
214 highly erodible materials. This inference is consistent with the presence of remnants of ancient impact craters  
215 that often characterize grooved terrains (fig. 7). Such remnants, commonly with positive relieves, suggest  
216 that they consist of rocks more resistant than the surrounding surfaces to the erosive processes shaping  
217 grooves. On the topmost part of remnants, grooves generally are absent or less prominent. Relationships  
218 among grooves and impact crater remnants, then, seem to confirm that that grooves formed mainly on  
219 relatively “soft” highly erodible materials.

220

#### 221 *4.1.3. Streamlined uplands*

222 Streamlined uplands occur both at the origin of Ares Vallis Complex troughs (i.e. in the vicinity of  
223 chaotic terrains), and at the terminal reach of Ares Vallis. They seem to have been formed by erosion of  
224 former Noachian and Early Hesperian plateau materials. Streamlined uplands are teardrop-shaped, and  
225 characterized by a whaleback profile. Their topmost part reaches the same altitude of the neighboring  
226 plateaus and consists of Noachian and Early Hesperian terrains (Pacifi, 2008). Usually, terrains  
227 surrounding streamlined uplands appear to be grooved.

228 Streamlined uplands located in the vicinity of chaotic terrains (fig. 8) are the most prominent features  
229 occurring near (and sometime in connection with) the flood source areas. Arrangement of such streamlined  
230 uplands indicates that they were shaped by broad converging floods coming out from the chaos. Cross-  
231 cutting relationships among troughs separating streamlined uplands seem to indicate that floods abandoned  
232 lateral troughs early with respect to the innermost ones. This setting could be consistent with a progressive

233 decreasing of the fluid level in the reservoirs during discharges, which resulted in a progressive canalization  
234 of floods.

235 Streamlined uplands occurring at the terminal reach of Ares Vallis (fig. 9) show a distribution and  
236 orientations suggesting a spreading of floods. The upstream portion of streamlined uplands is commonly  
237 characterized by an impact crater or a rocky hill, which is believed to have caused the diversion of flow,  
238 protecting downstream Noachian and Early Hesperian plateaus from flood erosion (fig. 10).

239

#### 240 *4.1.4 Giant Bars*

241 We observe a few features occurring in alcoves flanking valley floors on the downstream portion of  
242 Narrow Ares Vallis (fig. 11). They appear some kilometers long, a few km wide, and rising for about 500 m  
243 from the valley floor. We propose two hypotheses for the origin of such features. In the first hypothesis we  
244 observe that these features appear strikingly similar to giant eddy bars formed during some known terrestrial  
245 catastrophic floods in alcoves flanking flooded valleys (Carling et al., 2002). Thus we suggest that such  
246 Martian features could have been formed as giant bars during Ares Vallis catastrophic floods. Their  
247 thicknesses suggest that catastrophic flood(s) probably responsible for their emplacement was (were) at least  
248 500 m deep in the narrow reach of Ares Vallis. The origin of the alcove features could be related to  
249 exhumation and erosion of buried impact craters by catastrophic floods. These features overlie grooved  
250 terrains and are separated from the valley wall by a swath of about 1.5 km. Such separation can be  
251 interpreted as a non-deposition zone, which occurs between bedforms and valley walls, and which is  
252 interpreted to form by flow separation immediately downstream from a flow expansion or channel bend  
253 (Burr et al., 2004). The topmost part of the possible bars is almost flat and lacks grooves. It is possible to  
254 identify boulders about 5-10 m in diameter on the largest pristine impact crater (1.5 km in diameter)  
255 occurring on top of one the possible bar.

256 In the second hypothesis, we suggest that these features could be interpreted as mass wasting  
257 deposits originated by collapsing of Ares Vallis walls, and possibly reworked by following catastrophic  
258 floods. However, lacking of erosional features, such as grooves, and occurrence of the flat trough, which  
259 characteristically separates this feature from the valley wall, lead us to discard this second idea.

260

#### 261 *4.1.5 Pendant bars*

262 The term pendant bar was introduced to indicate streamlined mounds emplaced by Missoula floods  
263 downstream of bedrock projections in the Channeled Scabland of North America (Baker, 1982). Pendant  
264 bars form by sediment deposition in flow separations developing downstream from a flow obstacle. Similar  
265 features, kilometers long and hundreds of meters high, occur in the Ares Vallis Complex (fig. 12), mostly at  
266 the terminal reach of Ares Vallis. Pendant bars distinguish from streamlined uplands: the former, which are  
267 essentially depositional features, develop exclusively downstream of a bedrock projection, and appear  
268 noticeably thinner with respect to the bedrock; the latter, which are erosional morphologies, typically lack a  
269 bedrock projection on the upstream side (fig. 9b) or, if this occurs, both are about the same thickness (fig.  
270 10).

271 Using HRSC data, three-dimensional analyses were performed for two pendant bars (fig. 12), which  
272 are located in the Ares Vallis terminal reach (fig. 9a). Bedrock knobs occurring upstream of the pendant bars  
273 are about 3 km wide and 4 km long, and rise for about 500-600 m with respect to the nearest valley floor.  
274 Streamlined deposits forming bars are 20-35 km long, and their topmost parts rise for about 300-400 m. The  
275 upstream portion of Pb1 (fig. 12a, 12b) is surrounded by a parabolic-shaped scour, and the adjacent valley  
276 floor is extensively grooved. Both upstream parabolic scour and grooved terrain are not observed at the Pb2  
277 pendant bar (fig. 12c, 12d); the valley floor surrounding Pb2 consists of a flat deposit characterized by  
278 bright, shallow, and elongated hollows observable at the MOC NA resolution.

279 Our observations suggest that two different phases may have existed during each catastrophic flood  
280 event (fig. 12f). In the first phase, flood carved a parabolic scour upstream of bedrock projections and  
281 emplaced pendant bars to the downstream. At the same time, flood scoured grooves on the valley floor. The  
282 thicknesses of the pendant bars suggest that catastrophic flood in which they formed have a depth of at least  
283 about 300 m at the terminal reach of Ares Vallis. In the second phase during waning stage of catastrophic  
284 flood, the decreased strength of the flow led to the deposition of a flat sedimentary field in the inner part of  
285 channels, burying both parabolic scours and grooved terrains.

286 Some boulders are visible on the pendant bars as previously observed by Malin and Edgett (2001).  
287 However, a majority of boulders should have a smaller size range than can be observed in 1.5 m/pixel MOC  
288 NA images (fig. 12e). This boulder size range is similar to that of the largest boulders observed at the  
289 Pathfinder Landing site (Golombek et al., 1997), which is located next to the present-day termination of Ares

290 Vallis (fig. 9a). This fact could indicate that 1.5 m likely represents the upper limit of the dimension of clasts  
291 transported by Ares Vallis catastrophic floods at least at the terminal reaches and maybe during last floods.

292

293

#### 294 *4.1.6. Cataract-like features*

295 Abandoned cataracts are impressive erosional forms created during the Missoula catastrophic floods  
296 in North America. They were shaped by headwall recessional processes when catastrophic floods crossed a  
297 sharp scarp of structural or erosional origin (Baker, 1982). A very similar feature occurs at the Ares Vallis  
298 Complex near the junction of a shallow trough emanating from Western Valley and the Ares Vallis main  
299 trough (fig. 13). The shallow trough is hanging above both Western Valley and Ares Vallis floors: this  
300 suggests that it was carved early during the catastrophic flood event originated by fluids emanating from  
301 Hydaspis Chaos, and subsequently abandoned.

302 The cataract-like feature is an arcuate scarp, 500 m high and several kilometers wide. It seems to  
303 have originated when a catastrophic flood crossed a sharp scarp, and successively extended 35 km upstream  
304 by flood-driven, headwall recessional processes. Unlike terrestrial cataracts, large closed depressions are  
305 unobserved at the base of the cataract-like feature of the Ares Vallis Complex. The shallow trough occurring  
306 upstream of the cataract-like feature shows an association of grooved terrain, streamlined uplands and  
307 pendant bars. In the downstream of the cataract, instead, trough enlarges with a fan-shaped morphology: here  
308 grooved terrain and pendant bars are unobserved and only two small streamlined remnants occur.

309

## 310 **4.2. Ice-related morphologies**

### 311 *4.2.1 Thermokarstic depressions*

312 Shallow, irregularly-shaped depressions occur in several portions of the Ares Vallis Complex. They  
313 occur on erosional terraces, on valleys floors, and on top of ice-contact features (see next section). Several  
314 well-developed shallow depressions occur inside a large flat-floored impact crater about 90 km in diameter,  
315 which host a portion of Eastern Valley. We gave this impact crater an informal name of Eastern Valley  
316 Crater (fig. 14). Irregularly-shaped depressions of Eastern Valley Crater are a few kilometers wide, and  
317 typically coalescing. The depressions are 50–150 m deep. The deepest ones are coalescing and larger. The  
318 shallowest ones are smaller and isolated. The depression walls show layering (at least four) a few of tens of

319 meters thick (fig. 18). In its medial portion, the crater floor is incised by Eastern Valley. Nearby impact  
320 craters and intra-crater terrains do not exhibit shallow and coalescing depressions similar to those occurring  
321 within Eastern Valley Crater. This fact leads us to think that the formation of such features does not depend  
322 on regional geological and/or climatic events, but relates exclusively to the geological history of Eastern  
323 Valley Crater, and to the geological properties of its floor materials.

324 The shallow and coalescing depressions observed in the Ares Vallis Complex share several  
325 morphological similarities with terrestrial thermokarstic depressions, such as alas valleys. Alas valleys are  
326 periglacial morphologies that form in permafrost or ice-rich soils. Thawing of ground-ice leads to the  
327 formation of thaw lakes, which could coalesce with others and with a stream (Czudek and Demek 1970).  
328 Probable alas valleys and other thermokarstic depressions have been already observed and mapped in  
329 circum-Chryse outflow channels by some authors (Carr and Shaber, 1977; Costard and Baker, 2001; Costard  
330 and Kargel, 1995). Such morphologies are supposed to form on Mars even by localized enhanced  
331 sublimation instead of melting processes (Levy et al., 2005). Carr and Shaber (1977) note that characteristics  
332 of alas valley on Mars, with respect to terrestrial ones, may indicate a more uniform distribution of ice within  
333 the surface materials. This indicates that the ices were deposited contemporarily with the host material.

334 We hypothesize the following scenario (fig. 14) about the origin of the thermokarstic depressions in  
335 Eastern Valley Crater. Catastrophic flood(s) originated from Iani Chaos, etched the Eastern Valley Crater  
336 rim, and infilled it with ice-rich deposits. The layering observed in depression walls seems to indicate  
337 multiple occurrences of catastrophic flooding, or at least that variations in the flow regime existed. After the  
338 flood(s), an ice-rich deposit occupied the Eastern Valley Crater floor. The ice-rich deposit would have  
339 subsequently wasted by melting or sublimating processes, leading to the alas-like landscape. The depths of  
340 the thermokarstic depressions suggest a thickness of at least 150 m for the ice-rich deposit.

341 Eastern Valley incises through the thermokarstic depressions, implying at least two different flood  
342 events in the area: the earlier one(s) supplied the stratified ice-rich deposit; the later one(s) eroded it  
343 subsequently to the development of the thermokarstic depressions. During the later flood(s), processes of  
344 thermal erosion may have played an important role in the reworking of the ice-rich deposit. Thermal erosion  
345 causes degradation and removal of ice-rich soils by heat transfer between the water flow and the frozen  
346 ground, followed by transport of unfrozen materials (Aguirre-Puente et al., 1994).

347 The gap in time occurring between the earlier and later flood(s) must have been long enough to allow  
348 development of thermokarstic depressions and their coalescence. Brouchkov et al. (2004), based on the study  
349 of thermokarstic depressions in Central Yacutia, noted that active phase of a terrestrial thermokarst feature is  
350 short, and that its development should be considered a short-term event. Calculations of thermal conditions  
351 beneath a thermokarst lake in Central Yacutia show that, if the water level is stable or increasing, thaw may  
352 reach 30 m over a period of 200 years. If the ice-wasting processes responsible for the Martian alas-like  
353 depressions were dominated by melting rather than sublimation process, development of thermokarstic  
354 depressions may have been relatively fast (about some hundreds to a few thousand of years). Harris (2002)  
355 observe that a thaw pond, once formed, will go on enlarging in icy materials until it runs out of ground ice or  
356 intersect a drainage way. In the same way, it is possible that the last flood(s) through Eastern Valley partially  
357 disrupted walls of the alas-like depressions, caused their draining, and then stopped their development.

358 The overall setting of features observed in Eastern Valley Crater seems to imply alternation of  
359 periods characterized by colder-dryer climatic conditions (similar to the present-day Martian climate) in  
360 which ice-rich deposits were emplaced, and periods characterized by warmer-wetter climatic conditions in  
361 which alas-like features were shaped. The inference about the possible warmer-wetter climatic conditions  
362 may be invalid if sublimation rather melting processes dominated the wasting of the ice-rich deposits.  
363 Nevertheless, the geomorphological relationship between the alas-like valleys and the present-day Eastern  
364 Valley indicates that floods were multiple and well separated in time.

365

#### 366 *4.2.2. Ice-contact morphologies*

367 Patches of mesa-like features overlie erosional morphologies of the Ares Vallis Complex shaped by  
368 catastrophic flood processes. In the narrow upper reach of Ares Vallis, the mesa-like features are flat-topped  
369 ridges (fig. 15), a few of kilometers wide, tens of kilometers long, and rising for about 100-200 m. They are  
370 slightly sinuous, and elongated parallel to the trough. Locally, the ridges bifurcate and turn around  
371 streamlined hills. In the wide lower reach of Ares Vallis (fig. 16), the mesa-like features vary in shape,  
372 dimension or orientation. They exhibit forms such as circular, crescent, elongated, reticulated, bifurcating or  
373 sinuous. The thickest mesa-like features rise for about 500 m and occur in the upstream portion of Wide Ares  
374 Vallis. Toward the downstream direction, the thickness of the mesa-like features progressively decreases,  
375 until it reaches a value of about 100 m (fig. 2). The topmost portion of the largest mesa-like feature appears

376 to be etched by round-shaped, flat-floored depressions, which are consistent with a thermokarstic origin (fig.  
377 16a). At the bottom of such depressions, underlying grooved terrain and streamlined hills formed during  
378 catastrophic flood events are observed. Several mesa-like features are characterized by a rising sharp rim  
379 (fig. 16d). The mesas-like features lack any erosional marks such as grooves or terraces. Their walls are  
380 generally steep and layering is commonly recognizable. Layering is diverse in individual mesa-like feature or  
381 even on the different slopes of a mesa-like feature (fig. 16e).

382         Some morphological characteristics of the mesa-like features appear to be very similar to those of  
383 terrestrial kames, and thus they may have formed owing to similar geomorphic processes. Kames are steep-  
384 sided, variably shaped mounds, composed mainly of sands and gravels. They form because of emplacement  
385 of sediments in ice-walled streams or lakes, in sub-glacial, englacial or supraglacial environments. These  
386 features were left as rising morphologies when surrounding ice melted (Benn and Evans, 1998). Commonly  
387 shared features characterizing both the mesa-like features of Ares Vallis and terrestrial kames are; steep  
388 walls, flat topmost part, irregularly-shaped morphology, layered structure, variations in layering of individual  
389 mesa-like features. The rising rim characterizing some mesa-like features of Ares Vallis is somewhat similar  
390 to those characterizing terrestrial ice-walled lake plains, which formed by sediments that accumulated near  
391 the margin of ice-walled lakes (Johnson and Menzies, 1996). The mesas-like features showing a reticulated  
392 pattern can be considered to be a gigantic version of terrestrial disintegration ridges, which formed by  
393 infilling of crevasses and other openings in disintegrating ice (Flint, 1971).

394         Our interpretation of the Martian features as ice-contact deposits mostly agrees with one of those  
395 proposed by Costard and Baker (2001), and implies that one or more ice masses filled Ares Vallis.  
396 Occurrence of such features requires that ice masses were stagnant at least from the time during which the  
397 probable kame features were emplaced until the ice wasted. The varying thickness of the ice-contact features  
398 implies i) differences in ice mass thickness along Ares Vallis, ii) variation in the amount of materials  
399 emplaced against ice masses, and finally iii) that sediments forming the probable kame features were  
400 deposited in different times throughout the wasting of the ice masses.

401         The materials forming the probable kame features seem to have originated from Ares Vallis walls,  
402 and appear to have been emplaced by fluvial-like processes (fig. 17). The bifurcating ridge of fig. 15 shows  
403 an olivine-rich composition and thermal inertia values higher than other surfaces occurring in the  
404 neighboring areas (Rogers et al., 2005). Thermal inertia values appear to be compatible with gravel and sand

405 deposits, while the olivine-rich composition could be due to stream sorting processes. Indeed, olivine-rich  
406 layers occur on Ares Vallis walls (Rogers et al., 2005) and could represent source areas for sands and gravels  
407 forming the ridge.

408 Russell et al. (2001) describe a giant, supraglacial, ice-walled channel excavated into the snout of  
409 Skeiðarárjökull, Iceland, during the November 1996 jökulhlaup. The supraglacial channel was 500 m long,  
410 100 m wide and 40 m deep. Mean flow velocities of the jökulhlaup ranged between 7 and 11 m s<sup>-1</sup>, which  
411 were capable of suspending sediments with grain size up to 20 cm. Deposits occurring at the floor of the  
412 channel consist of an 8 meter thick succession of progradational and aggradational gravel macroforms.  
413 Russell et al. (2001) observe that, since the November 1996 jökulhlaup, ablation has lowered the surrounding  
414 glacier surface by approximately 30 m, and the ice-walled channel has become a prominent flat-topped ridge.  
415 This feature could be one of the most interesting terrestrial analogs for the ice-walled stream deposits of Ares  
416 Vallis.

417 Alternative geomorphological processes of landscape evolution seem to be less likely for explaining  
418 the mesa-like features. Stream deposits not involving ice-masses can form inverted topography such as those  
419 observed in Eberswalde Crater on Mars (Malin and Edget, 2003). However, the patterns of the mesa-like  
420 features in Ares Vallis do not present expected fluvial forms such as tributary and distributary patterns. Lava  
421 flows could account for the olivine-rich composition of some ridges. Although ice-dammed lavas could form  
422 steep-sided lava flows, volcanic features are not observed in this area. The layering observed in Ares Vallis  
423 mesa-like features could have resulted from different insolation occurring at different facing slopes, and/or  
424 variable climates, leading to dissimilar erosive and/or sedimentary processes, which at places could have  
425 masked or enhanced sediment layering.

426

#### 427 *4.2.3. Patterned terrains*

428 Terrains showing pitted or polygonal patterns appear in various reaches of the Ares Vallis Complex.  
429 They occur at the highest stratigraphical level, and thus their emplacement may represent the latest of main  
430 geological events shaping the Ares Vallis Complex.

431 Pitted terrains consist of surfaces dotted by numerous hollows. Larger pits are 100 m wide, whereas  
432 the smallest ones distinguishable are 10-20 m wide. Pits have a quasi-circular shape, and sometime tend to  
433 aggregate each other. Typically, they exhibit dark floor, and sand dunes are recognizable on the largest ones.

434 Patches of pitted terrains occupy floors of the Ares Vallis Complex and Eastern Valley Crater (fig. 18).  
435 Furthermore, pits characterize mass wasting deposits occurring along Ares Vallis walls (fig. 19). In THEMIS  
436 IR nighttime data, pitted terrains show higher emittance values than surrounding surfaces. Association of  
437 pitted pattern and thermal properties of such terrains appears remarkable. This association, together with the  
438 absence of pits on nearby terrains, leads us to hypothesize that pits formed because of soil properties, rather  
439 than alternative causes (e.g. primary or secondary impact craters).

440 Terrains showing polygonal pattern generally embay the probable kame features occurring on the  
441 inner and deeper portions of Ares Vallis (fig. 15 and 16). There polygons appear to be hundreds of meters  
442 large and peripheral trenches are tens of meters wide. In THEMIS IR nighttime data, polygonal terrains show  
443 emittance values higher than Ares Vallis walls and lower than probable kame features.

444 Both the pitted and polygonal terrains may have originated because of periglacial processes. On  
445 Earth, pitted patterns similar to those observed in the Ares Vallis Complex generally correlate with terrains  
446 subject to ground collapses due to thermokarstic processes. Possible terrestrial analogues are kettle-holes and  
447 thaw-lakes (Pacifici et al., 2005), which form when buried-ice or permafrost melts, forming pits on the  
448 surface. Polygonal terrains could have been formed also by desiccation processes. However, the occurrence  
449 of the probable kame features suggests that a periglacial origin is more likely. Melting of buried ice and  
450 upward movement of melt water could have originated ice cemented soils and duricrusts on Mars (Landis et  
451 al. 2004). Both ice-cemented soils and duricrusts could be responsible for the higher IR emittance values  
452 shown by patterned terrains with respect to surrounding surfaces.

453 The occurrence of geomorphological features related to periglacial processes, such as pitted and  
454 polygonal terrains, agrees with the hypothesis that ice masses filled the Ares Vallis Complex in the past.  
455 Moreover, periglacial features suggest that portions of the ice masses were buried after their emplacement.  
456 Processes responsible for ice burying may have been mass wasting, emplacement of impact crater ejecta, or  
457 wind-blown materials, such as dust, sand, and volcanic ash. A sublimation till could have buried ice as well,  
458 if the original ice mass contained some amount of debris. Sublimation till of Beacon Valley in Dry Valleys,  
459 Antarctica, shows a well-developed polygonal pattern (Marchant et al., 2002). Dry Valleys are known also as  
460 one of the best Martian analogues on Earth.

461

462

463

464 **5. Discussion**465 **5.1. Catastrophic floods**

466 Some of the erosional and depositional morphologies occurring in the Ares Vallis Complex, such as  
467 streamlined uplands, giant bars, pendant bars, and cataract-like features, suggest that Ares Vallis and its  
468 valley arms were shaped by catastrophic floods originating from chaos regions. This idea agrees with the  
469 previous hypothesis (Baker and Milton, 1974; Baker, 1982; Baker et al., 1992; Komatsu and Baker, 1997).

470 Our geomorphological analysis of high-resolution images estimates that flood events were at least  
471 six. Reactivation of outflow channel flooding is indicated also at Tiu Vallis west of Ares Vallis (Rodriguez et  
472 al., 2005), thus it can be concluded that large circum-Chryse outflow channels were commonly formed by  
473 multiple floods. Occurrence of multiple floods is in agreement with numerical model of groundwater flow  
474 and surface discharge at the outflow channel sources (Harrison and Grimm, 2008). Topographic analyses of  
475 giant and pendant bars indicate that floods were at least 500 m deep in Narrow Ares Vallis, and at least 300  
476 m deep at the Ares Vallis terminal reach. Geomorphological relationships indicate a progressive decreasing  
477 of fluid volume in the reservoirs during the discharges, which resulted in a progressive canalization of  
478 floods. This is partially in agreement with Nelson and Greeley (1999). Our hypothesis about the  
479 geomorphological evolution of Eastern Valley Crater (fig. 14) suggests that the amount of time elapsed  
480 between the two different floods in Eastern Valley must have been long enough to have permitted the  
481 emplacement of thermokarstic features 150 m deep and a few kilometres large. We do not know how much  
482 time was required for their formation. To make a roughly comparison, similar features 20 meters deep could  
483 require few hundreds of years to form on Earth (Brouckov et al., 2004). Occurrence of layering could  
484 suggest two hypotheses. On the first one, each layer, a few tens of meters thick, formed during different  
485 floods; in the second hypothesis we suggest that layering formed because of variations in the flow regime  
486 during a single flood. Both the hypotheses appear to be consistent.

487

488 **5.2. Grooved terrains**

489 Grooved terrains characterize a large portion of the Ares Vallis Complex floors and erosional  
490 terraces, and occur also at other Martian outflow channels, such as in Kasei Valles. In earlier works on  
491 Martian outflow channels, main interpretations of grooved terrains were: i) features sculpted by high-

492 velocity (catastrophic) flows of water (Baker and Milton, 1974) and ii) features similar to glacial scours and  
493 mega-flutes (Lucchitta, 1982; Lucchitta, 2001). In the former hypothesis grooves are considered to have been  
494 formed by powerful roller vortices, which developed parallel to the flow direction. In the latter hypothesis  
495 grooves are shaped by ice that in place moved through Martian channels. Ices flow similarly in Antarctic ice  
496 streams over deformable debris saturated with water under high pore pressure. Other hypotheses about  
497 groove origins including formation by roller vortices in fluids such as wind, debris flows and mudflows,  
498 were discussed in Baker et al. (1992) and Carr (1996). Origin of grooves could be inferred from geological  
499 relationships among grooves and nearby geomorphological features. In the Ares Vallis Complex, occurrence  
500 of cataract-like features, streamlined uplands, and pendant bars in association with grooved terrains (fig. 13)  
501 seems to support the cataclysmic flood origin.

502 Geomorphological characteristics of the observed grooves, and their relationship with respect to  
503 nearby features, such as meandering channels (fig. 6) and impact craters remnants (fig. 7), suggest that the  
504 grooves formed mainly on relatively “soft” highly erodible materials.

505 In areas where water flowed deeper and for longer durations (i.e., on the Ares Vallis floor) grooves  
506 appear wider and deeper than in the areas where water flowed shallower and for shorter times (i.e., in  
507 Western Valley). This appears in agreement with laboratory experiments and field observations. Laboratory  
508 experiments on water streams indicate that regular spacing of vortices in flow varies with velocity and depth  
509 of the flow (Allen, 1970). Field observations at the base of the Sigsbee Escarpment, in the northwestern Gulf  
510 of Mexico (Bean, 2003), show that strong currents formed mega-furrows on fine-grained sediments of  
511 seafloor. Higher current velocities and durations lead to form mega-furrow, which are wider, deeper and  
512 closer. Furthermore, the stronger sediments determine the maximum depth of erosion and require higher  
513 current velocity and duration to be eroded (Bean, 2003). Such seafloor mega-furrows exhibit some  
514 similarities with respect to Martian grooves. Therefore, it is possible that similar currents occurred at the  
515 bottom of Martian catastrophic floods. At the southern termination of Western Valley (fig. 4), grooves seem  
516 to converge and meet to form a deep and narrow canyon-like feature. This appears in agreement with some  
517 experimental flow simulations (Shepherd, 1972; Shepherd and Schumm, 1974) showing as the longitudinal  
518 grooves form early and finally switch to a deep inner channel that progressively extends backward.

519 On the other hand, some variations in trough geometry and consequent fluid properties seem not to  
520 have significantly influenced processes sculpting grooves. Several flow properties could have varied along

521 troughs, such as velocity, bedload quantity, granulometry density, fluid temperature, salt concentration, and  
522 amount of gases dissolved in the fluid. Martian grooves occur both in the proximity of the postulated fluid  
523 sources (fig. 8) and at the terminal reach of channels (fig. 9). This implies that grooves formed both in areas  
524 of convergence and divergence of floods, and in areas characterized by different topographic gradients (fig.  
525 2). Furthermore, the large extension of grooves implies that same flow conditions were sustained for very  
526 long distances, such as several hundreds of kilometers. In Western Valley, despite the large variations in  
527 width of the trough (fig. 4), grooves do not show significant variations both in morphology and in  
528 dimensions along the entire 370 km long valley. A more detailed discussion on the groove formation during  
529 flooding requires precise determinations of water depth and flow velocity in various reaches of Ares Vallis,  
530 possibly by utilizing numeral modeling (e.g., Miyamoto et al., 2006; 2007).

531

532 Lucchitta (2001) shows a remarkable similarity between Martian grooved terrains of Kasei Valles  
533 and glacial mega-lineations observed in sonar images of the sea floor in front of the Sea Ross Ice Shelf.  
534 Intrigued by this striking similarity, we have compared high-resolution images of grooved terrains of Ares  
535 Vallis with sonar images of terrestrial glacial mega-flutes occurring on the floor of the Ontario Lake (fig. 5).  
536 Martian grooves consist of narrow and elongated troughs, while terrestrial glacial mega-flutes consist of  
537 elongated ridges. However, the overall shapes, the dimensions, and the spatial distributions of terrestrial and  
538 Martian features appear to be very similar. Mega-flutes of the Ontario Lake floor consist of compact stony  
539 diamict (till) (Lewis et al., 1997). Similar mega-flute observed on seafloors was interpreted as soft, structure-  
540 less diamict (Dowdeswell et al., 2004), and subglacial till (Shipp and Anderson, 1997). Diamict and till are  
541 non-consolidated, poorly-sorted deposits: clasts vary from clay to boulders. Such kind of deposits could be  
542 similar to those forming some of Martian grooved terrains, which we interpret to consist of relatively “soft”  
543 highly erodible materials.

544

### 545 **5.3. Ice-covered catastrophic floods?**

546 Shaw (1996, 2002) proposed that terrestrial sub-glacial bedforms, such as those observed on the  
547 Ontario Lake floor, were shaped during the last ice age by enormous sub-glacial outburst floods. Sub-glacial  
548 floods are inferred to have formed meltwater sheets that flowed below ice masses producing mega-flutes,  
549 drumlins, tunnel valley and other sub-glacial bedforms. This theory is controversial (Benn and Evans, 1998),

550 and thus Kargel (2004) suggests that this fact is sufficient to give a pause to any rapid judgment about  
551 Martian outflow channels. The catastrophic floods sculpting Ares Vallis could have somehow evolved in  
552 conditions similar to those of a sub-glacial outburst floods. In fact, Wallace and Sagan (1979) propose that,  
553 under the present climatic condition of Mars, a flowing channel of liquid water would be covered by ice,  
554 which evaporates slowly enough to allow the water below to flow for distances up to hundreds of kilometers,  
555 even with quite modest discharges. They calculated that thickness of such ice-covers ranging from tens to  
556 several hundreds of meters, and that the amount of ice lost by evaporation at the top surface is replaced by  
557 freezing at the bottom surface. This implies that the net loss is to the liquid water. Several factors could  
558 enhance or reduce the thickness of such ice-covers. These are: i) temperature of water in the reservoirs; ii)  
559 amount of possible salts and gases eventually dissolved in water; iii) composition and temperature of Martian  
560 atmosphere, and presence of atmospheric clouds or dusts; iv) possible different obliquity of Martian axis  
561 (Laskar and Robutel, 1993). Lucchitta (1982) proposed that in the cold Martian climate water coming from  
562 chaos regions was supercooled and then acquired rapidly large quantities of frazil ice, which locally may  
563 have developed ice caps. Some authors (Harrison and Grimm, 2008 and therein) suggest that in most cases  
564 groundwater discharge at chaotic terrain did not provide a direct source of channel flow but ponded locally  
565 and produced standing bodies of water; successively, outflow channel floods were triggered by jökulhlaup-  
566 type events caused by failure of the lake margins. In this case, if ice masses formed on top of standing bodies  
567 of water, they could have been carried by catastrophic floods. Therefore, the formation of ice jams near  
568 obstacles and constrictions could have happened, successively followed by consolidation to form ice masses  
569 (Lucchitta, 1982). It is possible, then, that floods flowing in the Ares Vallis Complex could have provided  
570 enough ice to generate one or more ice masses hundreds of meters thick. Evidence for ice-rich deposits  
571 overlying catastrophic flood morphologies was observed in the Mangala Valles outflow channel (Levy et al.,  
572 2005). Observation of such deposit draped over grooved terrain suggests to these authors that ice would have  
573 formed on top of an outflow flood under cold-dry climatic condition.

574         If floods were ice-covered, they could evolve into a setting similar to a relatively thin water sheet  
575 flooding below an ice-cover, at least during their waning stage. In such condition, water flowing under the  
576 ice masses could have shaped grooved terrains, by processes similar to those proposed by Shaw (2002),  
577 and/or could have enhanced grooves already carved by roller vortices of catastrophic floods. Furthermore, in  
578 such sub-ice circumstances, it is possible that catastrophic floods maintained the same flow condition for

579 very long distances, both in areas of converging and diverging flow (such as at the beginning and at the  
580 termination of Ares Vallis), and regardless of variations in width and depth of troughs. Possibly, small  
581 movements of ice cover may have occurred at the end of floods during the grounding of ice masses. This  
582 could have both enhanced or smoothed the previously shaped grooves.

583

#### 584 **5.4. Glacial landscape**

585 Our geomorphological analyses point out that ice masses grounded on the Ares Vallis Complex  
586 floors subsequent to multiple catastrophic floods, forming one or more dead-ice bodies, and formed glacial  
587 landscapes. It appears very probable that tremendous erosive action of each catastrophic flood should have  
588 totally removed ice masses and possible glacial and periglacial features produced after previous flood events.  
589 At the present day, a glacial landscape formed following the last catastrophic flood event is still visible. They  
590 consist of ice-contact features and thermokarstic depressions. Arrangement of such morphologies allows us  
591 to perform a rough estimation of the areas covered by ice-masses. In the case of Wide Ares Vallis where  
592 probable kame features appear densely occurring, assuming that these features formed in a single ice mass,  
593 the final reach of Ares Vallis was infilled by a dead ice-mass as large as  $3 \times 10^4 \text{ km}^2$ . They varied in thickness  
594 between 100 to 500 m. For the entire Ares Vallis Complex, the amount of ice infilling troughs should have  
595 been much higher than this value.

596 Evidence for a glacial landscape is absent in Western Valley. This may be due to the fact that  
597 Western Valley seems to have been carved by only one catastrophic flood. And the glacial landscape  
598 (possibly) emplaced at the end of such flood may have totally sublimate/melted without subsequent  
599 reworking. It is also possible that Western Valley was flooded for a brief time, or during warmer-wetter  
600 climatic conditions (see below), and then the resulting ice-cover was thinner than in other valleys. Finally, it  
601 is possible that fluid emanating from Hydaspis Chaos could have had a different temperature and/or  
602 composition in salts with respect to those of Iani and Aram Chaos, and then emplaced a thinner ice mass.

603 In the current Martian environment, ice once grounded could remain in place for a long time before  
604 totally sublimating or melting. Both morphological analyses (Levy et al., 2005) and models (Clifford and  
605 Parker, 2001) suggest this situation. In such an environment, ice masses could have preserved underlying  
606 grooved terrains from erosion, and could have favored consolidation of loose materials at their base. The  
607 pristine appearance of the grooved terrains and probable kame features in the Ares Vallis Complex may

608 suggest that ice masses disappeared mainly by sublimation processes, not by melting. Regarding the  
609 efficiency of sublimation processes on Mars, Clifford and Parker (2001) suggest that at latitudes lower than  
610  $40^\circ$ , which is the case of Ares Vallis, sublimation rates from a bare ice surface could readily exceed  $0.1 \text{ m yr}^{-1}$ .  
611 However, the presence of a debris mantle only 10-20 cm thick could reduce the sublimation rates by more  
612 than one order of magnitude. Considering both these end-members, the time required to sublimate a 500 m  
613 thick stagnant ice mass varies from 5000 to 50000 years, respectively in cases of bare and mantled ice.  
614 Mantling of ice could have been caused by emplacement of wind-blown sand, dust, volcanic ash, slope  
615 failure materials and impact crater ejecta. If the dead-ice masses contained some amount of debris, which is  
616 possible because of its origin, a sublimation till could have developed as well, lowering ice sublimation rate.  
617 Patterned terrains of the Ares Vallis Complex, and their thermal properties, suggest that periglacial processes  
618 occurred, and support the idea that ice was mantled or mixed with debris.

619         Periods of high or low obliquity of Mars, if occurred, could have increased or decreased ice  
620 sublimation rate. Observation of thermokarstic features, probable kame features, and relatively small-scale  
621 meandering channels, which seem to have been formed subsequent to multiple catastrophic flood events,  
622 suggests that relatively brief periods of warmer-wetter climatic conditions took place (see below), which  
623 could have favored melting rather than sublimation processes.

624

## 625         **5.5. Climatic changes**

626         Some morphological features of the Ares Vallis Complex are interpreted as formed by flowing or  
627 standing bodies of water in equilibrium with the Martian atmosphere. Such features are i) narrow,  
628 meandering channels, ii) thermokarstic features, and iii) probable kame features. Development of such  
629 features requires that periods of warmer-wetter climatic conditions took place. Thermokarstic features (fig.  
630 14) and hanging channels (fig. 13 and fig. 15) formed both on erosional terraces and icy deposits shaped by  
631 floods, and were modified by subsequent floods deepening troughs. This suggests that they developed  
632 between different catastrophic flood events. We hypothesize that such warmer-wetter climatic conditions  
633 were triggered by catastrophic flood events themselves. In fact, water vapor and carbon dioxide/methane  
634 gases liberated into the Martian atmosphere by degassing during outflow events could have induced a short-  
635 term greenhouse effect (Baker et al., 1991; Gulick et al., 1997; Baker, 2001). Water vapor released by  
636 wasting of stagnant ice-masses could have also sustained the greenhouse effect.

637 The pristine morphologies characterizing glacial and periglacial features of the Ares Vallis Complex  
638 may suggest that, in spite of the earlier warmer-wetter conditions, the main wasting of ice masses was driven  
639 by sublimation processes. This implies that the warmer-wetter climatic conditions occurred for relatively  
640 brief spans of time. Subsequently, climatic conditions became similar to those of the present day. Our  
641 observations agree with Baker (2001), which proposed that a short-duration, transient, warmer-wetter period  
642 followed the activation of catastrophic floods, and that afterward the Martian climate comes back to climatic  
643 conditions similar to those of the present day.

644

## 645 **6 – Conclusion**

646 The Ares Vallis Complex is one of the longest and ancient systems of outflow channels on Mars.  
647 Some of its morphological features (i.e. grooved erosional terraces, streamlined uplands, pendant bars, and  
648 cataract-like features) appear to have originated by multiple, time-scattered, catastrophic floods. Other  
649 morphological features (i.e. probable kame features, thermokarstic depressions, and patterned terrains)  
650 indicate that Ares Vallis hosted dead-ice masses in the past. Geological relationships between the  
651 catastrophic flood features and the ice-related features depict a possible geological evolution of Ares Vallis,  
652 involving a cyclic series of geomorphic processes (fig. 20) consisting of i) multiple, ice-covered catastrophic  
653 floods; ii) grounding of ice-masses formed on top of floods; iii) emplacement of ice-contact deposits, and  
654 finally iv) ice wasting.

655 A possible geological history of Ares Vallis is here summarized.

656 i) The Ares Vallis Complex originated by enormous floods discharged from chaotic terrains. The  
657 floods were responsible for sculpting grooved terrains, erosional terraces, streamlined uplands, and giant  
658 cataract-like features. The grooved terrains formed both at the proximal and at the distal reaches of the Ares  
659 Vallis Complex, and were originated by powerful vortices at the base of the enormous floods. Grooves  
660 formed prevalently on relatively erodible “soft” terrains, and their dimensions seem to vary depending on  
661 thickness and duration of the floods. Depositional features emplaced by floods consist of giant bars and  
662 pendant bars.

663 ii) Ice-covers formed on top of floods because of low values of temperature and pressure of Martian  
664 atmosphere. The amount of ice lost by evaporation at the top surface reformed by freezing at the bottom  
665 surface, allowing the ice-cover to thicken up to several tens to few hundreds of meters. As the floods

666 decreased their discharges, this setting evolved into a thick ice mass topping a relatively thin layer of flowing  
667 water. In such conditions, subglacial floods contributed to or enhanced sculpting of grooves.

668         iii) At the end of the floods, ice-covers grounded on the valley floor, forming thick, dead-ice masses.  
669 The ice masses could have taken a long time to totally waste (about a few thousand to a few tens of thousand  
670 of years, respectively in case of bare and debris mantled ice). Warmer-wetter climatic conditions prevailed  
671 during the first stage of wasting of the ice, and streams of water etched ice masses forming ice-walled  
672 channels and lakes. Origin of such water streams seems to be related to melting of permafrost and/or ice. The  
673 warmer-wetter climatic conditions were triggered probably by the greenhouse effect caused by water vapor  
674 and carbon dioxide/methane gases released during the catastrophic flood processes. If catastrophic flood  
675 events occurred during the warmer-wetter climatic conditions, it is plausible that they were ice free.

676         iv) Finally, ice masses totally wasted. Ice wasting produced a landscape inversion and materials  
677 deposited at the floor of ice-walled channels and lakes turn into mesa-like features, similarly to terrestrial  
678 kame deposits. Pristine appearance of sub-glacial and supra-glacial features (i.e. grooved terrains and  
679 probable kame features, respectively) suggests that colder-drier conditions prevailed during the second stage  
680 of dead-ice mass wasting. This leads us to think that the greenhouse effect persisted no longer than the time  
681 required to totally waste the ice masses infilling Ares Vallis.

682         Quantitative geomorphological analysis, realized by using high-resolution images and HRSC stereo-  
683 derived DTMs, allowed us to estimate some parameters about catastrophic floods and glacial masses. At  
684 least six catastrophic floods originated in Iani Chaos and sculpted Ares Vallis, at least two (probably more)  
685 originated in Aram Chaos. Water emanating from Hydaspis Chaos fed the Ares Vallis Complex during one  
686 single catastrophic flood event. On the narrow reach of Ares Vallis, floods had a minimum depth of about  
687 500 m, estimated on the base of thicknesses of giant bars. In Wide Ares Vallis, instead, thicknesses of  
688 pendant bars suggest a minimum depth of about 300 m. Arrangement of ice-related features and their  
689 thicknesses allow estimating the minimum aerial extent and thickness of the ice-mass(es) in which they  
690 formed. Ice mass(es) was one to five hundreds of meters thick and tens of thousand of square kilometers in  
691 area.

692         Throughout the wasting period of dead-ice mass(es), ice were locally buried by mass wasting  
693 processes, wind-blown materials, debris flows, and possibly by sublimation till. Periglacial processes acting  
694 on the buried ice formed patterned terrains and ice-cemented soils.

695

696

697

698

699

700

701

702 **Acknowledgement:**

703 We would like to thank Professor V.R. Baker for its helpful suggestions and comments. We thank the HRSC  
704 Experiment Teams at DLR Berlin and Freie Universitaet Berlin as well as the Mars Express Project Teams at  
705 ESTEC and ESOC for their successful planning and acquisition of data as well as for making the processed  
706 data available to the HRSC Team. We acknowledge the effort of the HRSC Co-Investigator Team members  
707 and their associates who have contributed to this investigation in the preparatory phase and in scientific  
708 discussions within the Team. We would like to thank for the reviews by Keith Harrison and Cathy Quantin,  
709 which greatly improved this work with suggestions and observations. This research was supported by  
710 Agenzia Spaziale Italiana.

711

712 **References**

713 Allen, J.R.L., 1970. Physical Processes of sedimentation. American Elsevier, New York.

714

715 Aguirre-Puente, J., Costard, F., Posado-Cano, R., 1994. Contribution to the study of thermal erosion on  
716 Mars. *J. Geophys. Res.* Vol.99 (E3), 5657-5667

717

718 Baker, V.R., 1982. The Channels of Mars. Univ. of Texas Press, Austin.

719

720 Baker, V.R., 2001. Water and the Martian landscape. *Nature*, 412, 228-236.

721

722 Baker, V.R., Milton, D.J., 1974. Erosion by Catastrophic Floods on Mars and Earth. *Icarus*, 23, 27-41.

723

- 724 Baker, V.R., Strom, R.G., Gulick, V.C., Kargel, J.S., Komatsu, G., Kale, V.S., 1991. Ancient oceans, ice  
725 sheet and the hydrological cycle on Mars. *Nature*, 352, 589-594.  
726
- 727 Baker, V.R., Carr, M.H., Gulick, V.C., Williams, C.R., Marley, M.S., 1992. Channels and valley networks.  
728 In: Kieffer, H.H., Jakosky, B.M., Synder, C.W., Matthews, M.S. (Eds.), *Mars*. University of Arizona  
729 Press, Tucson, pp. 483-522.  
730
- 731 Bean, D.A., 2003. Characteristics of mega-furrows on the continental rise seaward of the Sigsbee  
732 Escarpment, Gulf of Mexico. In: *Depositional processes and characteristics of siltstones, mudstones  
733 and shales*. SEPM ( Society for Sedimentary Geology).  
734
- 735 Benn, D.I., Evans, D.J.A., 1998. *Glaciers & glaciation*. Arnold, London.  
736
- 737 Brouchkov, A., Fukuda, M., Fedorov, A., Konstantinov, P., Iwahana, G., 2004. Thermokarst as a Short-term  
738 Permafrost Disturbance, Central Yacutia. *Permafrost and Periglac. Process.* 15, 81-87.  
739
- 740 Burr, D.M., Carling P.A., Beyer, R.A., Lancaster, N., 2004. Flood-formed dunes in Athabasca Valles, Mars:  
741 morphology, modeling, and implications. *Icarus*, 171, 68–83.  
742
- 743 Carling, P.A., Kirkbride, A.D., Parnachov, S., Borodavko, P.S., Berger, G.W., 2002. Late quaternary  
744 catastrophic flooding in the Altai Mountains of south-central Siberia: a synoptic overview and an  
745 introduction to flood deposit sedimentology. *Spec. Publ. Int. Ass. Sediment.* 32, 17-35.  
746
- 747 Carr, M.H., 1996. *Water on Mars*. Oxford University Press, Inc. New York.  
748
- 749 Carr, M.H., Shaber, G.G., 1977. Martian Permafrost Features. *J. Geophys. Res.* 82 (28), 4039-4054  
750
- 751 Clifford, S.M., Parker, T.J., 2001. The evolution of the Martian hydrosphere: implication for the fate of a  
752 primordial ocean and the current state of the northern plains. *Icarus*, 154, 40-79.

753

754 Costard, F., 1989. Fluvio-thermal erosion on Mars: a siberian analogy. *Lunar and Planet. Sci.* XX, 189-190.

755

756 Costard, F., Dollfus, A., 1986. Ice lenses on Mars. *Lunar and Planet. Sci.* XVII

757

758 Costard, F.M., Kargel, J.S., 1995. Outwash Plains and Thermokarst on Mars. *Icarus*, 114, 93-112

759

760 Costard, F., Baker, V.R. 2001. Thermokarst landform and processes in Ares Vallis, Mars. *Geomorphology*,

761 37, 289-301.

762

763 Czudek, T., Demek, J., 1970. Thermokarst in Siberia and its influence on the development of lowland relief.

764 *Quaternary Res.*, 1, 103-120.

765

766 Dowdeswell, J.A., Ó Cofaigh, C., Pudsey, C.J., 2004. Thickness and extent of the subglacial till layer

767 beneath an Antarctic paleo-ice stream. *Geology*, 32 (1), 13-16.

768

769 Flint, R.F., 1971. *Glacial and quaternary geology*. Wiley, New York.

770

771 Glicken, H., Schultz P.H., 1980. Martian Channel Erosion: The lahar analogy. *Lunar and Planet. Sci.* XI,

772 330-332.

773

774 Golombek, M.P., Cook, R.A., Economou, T., Folkner, W.M., Haldemann, A.F.C. , Kallemeyn, P.H.,

775 Knudsen, J.M., Manning, R.M., Moore, H.J., Parker, T.J., Rieder, R., Schofield, J.T., Smith, P.H.,

776 Vaughan, R.M., 1997. Overview of the Mars Pathfinder Mission and Assessment of Landing Site

777 Predictions. *Science*, 278, (5344), 1743 - 1748.

778

779 Gulick, V.C., Tyler, D., McKay, C.P., Haberle, R.M., 1997. Episodic ocean-induced CO<sub>2</sub> Greenhouse on

780 Mars: Implications for fluvial valley formation. *Icarus*, 130, 68-86.

781

- 782 Harris, S.A., 2002. Causes and Consequences of Rapid Termokarst Development in Permafrost or Glacial  
783 Terrain. *Permafrost and Periglac. Process.*, 13, 237-242.  
784
- 785 Harrison, K. P., Grimm, R.E., 2008. Multiple flooding events in Martian outflow channels. *J. Geophys. Res.*,  
786 113, E02002, doi:10.1029/2007JE002951.  
787
- 788 Hartmann, W.K., 2005. Martian cratering 8: Isochron refinement and the chronology of Mars. *Icarus*, 174,  
789 294-320.  
790
- 791 Johnson, W.H., Menzies, J., 1996. Pleistocene Supraglacial and ice-marginal deposits and landforms. In:  
792 Menzies, J. (Ed), *Past Glacial Environments: Sediments, Forms and Techniques - (Glacial*  
793 *Environments Series; 2)*, Butterworth-Heinemann, Oxford, pp. 137-160.  
794
- 795 Johnson, M.D., Mickelson, D.M., Clayton, L., Attig, J.W., 1995. Composition and genesis of glacial  
796 hummocks, western Wisconsin, USA. *Boreas*, 24, 97-116.  
797
- 798 Kargel, S.J., 2004. *Mars - A Warmer, Wetter Planet*. Springer Praxis Books / Space Exploration.  
799
- 800 Komatsu, G., Baker, V.R., 1997. Paleohydrology and flood geomorphology of Ares Vallis. *J. Geophys. Res.*,  
801 102 (E2), 4151-4160.  
802
- 803 Landis, G.A., Blaney, D., Cabrol, N., Clark, B.C., Farmer, J., Grotzinger, J., Greeley, R., McLennan, S.M.,  
804 Richter, L., Yen, A., and the MER Athena Science Team, 2004. Transient liquid water as a  
805 mechanism for induration of soil crust on Mars. *Lunar and Planet. Sci.* XXXV.  
806
- 807 Laskar, J., Robutel, P., 1993. The chaotic obliquity of the planets. *Nature*, 361, 608-612.  
808
- 809 Leverington, D.W., 2004. Volcanic rilles, streamlined islands, and the origin of outflow channels on Mars. *J.*  
810 *Geophys. Res.*, 109 (E10), 1-14

811

812 Levy J.S., Head, J.W., Marchant, D.R., Kreslavsky, M. 2005. Evidence for remnats of late Hesperian ice-rich  
813 deposits in the Mangala Valles outflow channel. *Lunar and Planet. Sci.* XXXVI.

814

815 Lewis, C.F.M., Mayer, L.A., Cameron, G.D.M., Todd, B.J., 1997. Drumlins in Lake Ontario. In Davies, T.  
816 A., Bell, T., Cooper, A.K., Josenhans, H., Polyak, L., Solheim, A., Stoker, M.S., Stravers, J.A.,  
817 (Eds), *Glaciated continental margins: an atlas of acoustic images*. Chapman & Hall, London, pp. 48-  
818 49.

819

820 Luchitta, B.K., Anderson, D.M., Shoji, H., 1981. Did ice streams carve martian outflow channels?. *Nature*,  
821 290, 759-763.

822

823 Lucchitta, B.K., 1982. Ice Sculpture in the Martian Outflow Channels. *J. Geophys. Res.*, 87, 9951-9973.

824

825 Lucchitta, B.K., 2001. Antarctic Ice Stream and Outflow Channels on Mars. *Geophys. Res. Letters.*, 28 (3),  
826 403-406.

827

828 Malin, M.C., Edgett, K.S., 2001. Mars Global Surveyor Mars Orbiter Camera: Interplanetary cruise through  
829 primary mission. *J. Geophys. Res.*, 106 (E10), 23,429-23,570.

830

831 Malin, M.C., Edgett, K.S., 2003. Evidences of persistent flow and aqueous sedimentation on early Mars.  
832 *Science*, 302, 1931-1934.

833

834 Mangold, N., Allemand, P., Thomas, P.G., 1998. Wrinkle ridges of Mars: structural analysis and evidence  
835 for shallow deformation controlled by ice-rich décollement. *Planet. Space Sci.*, 46 (4), 345-356.

836

837 Marchant, D.R., Lewis, A.R., Phillips, W.M., Moore, E.J., Souchez, R.A., Denton, G.H., Sugden, D.E.,  
838 Potter, N. Jr., Landis, G.P., 2002. Formation of patterned ground and sublimation till over Miocene  
839 glacier ice in Beacon Valley, southern Victoria Land, Antarctica. *GSA Bulletin*, 114 (6), 718.

840

841 Marchenko A.G., Basilevsky A.T., Hoffmann, H., Hauber, E., Cook, A.C., Neukum, G., 1998. Geology of  
842 the common mouth of the Ares and Tiu Valles, Mars. *Solar System Res.*, 32 (6), 425-452.

843

844 Miyamoto, H., Itoh, K., Komatsu, G., Baker, V.R., Dohm, J.M., Tosaka, H., Sasaki, S., 2006. Numerical  
845 simulations of large-scale cataclysmic floodwater: A simple depth-averaged model and an illustrative  
846 application. *Geomorphology* 76, 179–192.

847

848 Miyamoto, H., Komatsu, G., Baker, V.R., Dohm, J.M., Itoh, K., Tosaka, H., 2007. Cataclysmic Scabland  
849 flooding: Insights from a simple depth-averaged numerical model. *Environmental Modelling and*  
850 *Software* 22, 1400–1408, doi:10.1016/j.envsoft.2006.07.006.

851

852 Nelson, D.M., Greeley, R., 1999. Geology of Xanthe Terra outflow channels and the Mars Pathfinder  
853 landing site. *J. Geophys. Res.*, 104 (E4), 8653-8669.

854

855 Pacifici, A., 2008. Geomorphological map of Ares Vallis, Mars - ASI Planetary Map Series – Map n° 1.  
856 *Boll.Soc.Geol.It. (Ital.J.Geosci.)*, 127 (1), 75-92.

857

858 Pacifici, A., Ori, G.G., Neukum, G., and the HRSC Co-Investigator team, 2005. High-resolution  
859 morphological analysis of the central part of Ares Vallis using HRSC, MOC and THEMIS data. First  
860 Mars Express Science Conference.

861

862 Robinson, C.A., Neukum, G., Hoffmann, H., Marchenko, A., Basilevsky, A.T., Ori, G.G., 1996. A suggested  
863 geological development for Ares Vallis, Mars. *Lunar and Planet. Sci.* XXVII.

864

865 Rodriguez, J.A.P., Sasaki, S., Kuzmin, R.O., Dohm, J.M., Tanaka, K.L., Miyamoto, H., Kurita, K., Komatsu,  
866 G., Fairén, A.G., Ferris, J.C., 2005. Outflow channel sources, reactivation, and chaos formation,  
867 Xanthe Terra, Mars. *Icarus*, 175, 36-57.

868

869 Rogers, A.D., Christensen, P.R., Bandfield, J.L., 2005. Compositional heterogeneity of the ancient Martian  
870 crust: Analysis of Ares Vallis bedrock with THEMIS and TES data. *J. Geophys. Res.*, 110, E05010,  
871 doi:10.1029/2005JE002399.

872

873 Russel, A.J., Knudsen, Ó., Fay, H., Marren, P.M., Heinz, J., Tronicke, J., 2001. Morphology and  
874 sedimentology of a giant supraglacial, ice-walled, jökulhlaup channel, Skeiðarárjökull, Iceland:  
875 implications for esker genesis. *Global and Planetary Change*, 28, 193-216.

876

877 Shaw, J., 1996. A meltwater model for Laurentide subglacial landscape. In : McCann, S.B., Ford, D.C.,  
878 (Eds.), *Geomorphology sans Frontière*. Wiley, Chichester, pp. 182-226.

879

880 Shaw, J., 2002. The meltwater hypothesis for subglacial bedforms. *Quaternary International*, 90, 5-22.

881

882 Shepherd, R.G., 1972. Incised River Meanders: Evolution in Simulated Bedrock. *Science*, 178 (4059), 409-  
883 411

884

885 Shepherd, R.G., Schumm, S.A., 1974. Experimental Study of River Incision. *GSA Bulletin*, 85 (2), 257-268

886

887 Shipp, S., Anderson, J.B., 1997. Drumlin Field on the Ross Sea Continental Shelf, Antarctica. In Davies, T.  
888 A., Bell, T., Cooper, A.K., Josenhans, H., Polyak, L., Solheim, A., Stoker, M.S., Stravers, J.A.,  
889 (Eds), *Glaciated continental margins: an atlas of acoustic images*. Chapman & Hall, London, pp. 52-  
890 53.

891

892 Sudgen, D.E., Marchant, D.R., Potter, N.Jr., Souchez, R.A., Denton, G.H., Swisher, C.C.III., Tison, J., 1995.  
893 Preservation of Miocene glacier ice in East Antarctica. *Nature*, (376), 412-414.

894

895 Tanaka, K.L., 1997. Sedimentary history and mass flow structures of Chryse and Acidalia Planitiae, Mars. *J.*  
896 *Geophys. Res.* 102 (E2), 4131-4149

897

898 Tanaka, K.L., 1999. Debris-flow origin for the Simud/Tiu deposit on Mars. *J. Geophys. Res.*, 104 (E4), 8637  
899 -8651.

900

901 Tanaka, K.L., Skinner, J.A., Hare, T.M., 2005. Geologic Map of the Northern Plains of Mars. U.S.  
902 Geological Survey Scientific Investigations Map 2888, [available on World Wide Web at  
903 <http://pubs.usgs.gov/sim/2005/2888/>].

904

905 Werner, S., 2005. Major Aspects of the Chronostratigraphy and Geologic Evolutionary History of Mars.  
906 Ph.D. thesis, Freie Universität, Berlin.

907

908 Wallace, D., Sagan, C., 1979. Evaporation of ice in planetary atmospheres: Ice-covered rivers on Mars.  
909 *Icarus*, 39, 385-400.

910

911

912

913

914

915

916 **Figure captions**

917

918 Fig. 1. Location map of Ares Vallis Complex area based on the MOLA grid data. Frames refer to other  
919 figures.

920

921 Fig. 2. Longitudinal profile of Ares Vallis obtained from MOLA grid data. Notice the lowest portion of the  
922 valley resides in the narrow reach. Arrows indicate merging points of main valley arms debouching on Ares  
923 Vallis.

924

925 Fig. 3. Upstream reach of Ares Vallis. Arrangement of erosional terraces and streamlined uplands shows  
926 that at least six main catastrophic flood events sculpted Ares Vallis. The terrace formed during the first  
927 catastrophic flood event shows relative shallow anastomosing channels. Erosional terraces marking  
928 subsequent floods illustrate the progressive deepening and channelization of Ares Vallis. Frames refer to  
929 other figures. Mosaic of HRSC h0934\_0000, h0923\_0000, and h0912\_0000 images; topographic profile  
930 obtained from HRSC DTM mosaic.

931

932 Fig. 4. Western Valley topography from MOLA grid data. Arrows indicate flow directions as suggested from  
933 morphological features. Transversal topographic profile (AB) illustrates that Western Valley appears to be  
934 characterized by an elevated width-to-depth ratio (vertical exaggeration of profile is four times). Double-  
935 arrowed bar indicates lateral extension of grooved terrain. Frames refer to other figures.

936

937 Fig. 5. Grooves characterizing floors and erosional terraces of the Ares Vallis Complex consist of equally  
938 spacing furrows or trenches between narrow ridges. The most morphologically similar features observed on  
939 Earth are the glacial mega-flutes. a) Martian grooves; image MOC R1101630. b) Close up. c) Martian  
940 grooves; image THEMIS V12795005. d) Mega-flutes on sonar image of the Ontario Lake floor; reprinted  
941 from Quaternary International, Vol. 90, J. Shaw, The meltwater hypothesis for subglacial bedforms, Pages  
942 No 5-22, Copyright (2002), with permission from Elsevier. e) Mega-flutes on sonar image of the Ontario  
943 Lake floor; modified from Glaciated continental margins: an atlas of acoustic images. Chapman & Hall,  
944 London, 1997.

945

946 Fig. 6. Three-dimensional view of a portion of Western Valley and Aram Chaos rim; HRSC h1000\_0000  
947 image draped on HRSC DTM. See fig. 4 for location. a) The narrow outlet channel emanating from a 50 km  
948 wide impact crater located on the extended rim of Aram Chaos meets the central portion of Western Valley.  
949 Comparison between the channel 100-250 m deep and the grooves allows hypothesizing that the grooves are  
950 no more than some meters or a few tens of meters deep. b) At its downstream portion, the meandering  
951 channel etches the grooved floor of Western Valley and appears truncated by a shallow, small, chaotic  
952 region. c) The meandering channel does not show variations in proximity of the transition from the grooved  
953 to the non-grooved terrain, suggesting that geological properties of grooved and not-grooved terrains are

954 similar. d) HRSC h1000\_0000 and MOC E0900989 images mosaic showing a close-up of channel and its  
955 abandoned meanders.

956

957 Fig. 7. Impact crater remnants (black arrows) on the erosional terraces of Ares Vallis. Absence of grooves on  
958 the topmost part of the remnants suggests that grooves form mainly on relatively “soft” erodible materials.  
959 Notice the annular furrows embaying crater remnants. HRSC h1066\_0000 image. See figure 16 for a context  
960 image.

961

962 Fig. 8. Western Valley proximal reach in the vicinity of Hydaspis Chaos; see fig. 4 for location. This area  
963 consists of a fan-shaped system of broad, shallow, and grooved channels, which converge and meet together  
964 in the downstream. Higher parts of streamlined uplands appear to be flat and non-grooved. Lower parts  
965 appear to be grooved. Arrangement of grooves and streamlined uplands, and crosscutting relationships  
966 among channels, indicate an overall converging pattern of floods. HRSC h1022\_0000 image.

967

968 Fig. 9. a) Three-dimensional view of terminal reach of Ares Vallis; HRSC h1619\_0000 image draped on  
969 MOLA grid data. This portion of the valley is characterized by streamlined uplands (Su) and pendant bar  
970 (Pb1, Pb2, and Pb3). (P) indicates the Mars Pathfinder landing site. b) Probable kame features (M) clearly  
971 overlie a streamlined upland (Su); HRSC h01980\_0000 image draped on HRSC DTM.

972

973 Fig. 10. Streamlined uplands at the terminal reach of Ares Vallis. a) In areas of diverging floods, streamlined  
974 uplands commonly show an impact crater (C) on their upstream portion. Grooves characterize valley floor  
975 surrounding streamlined uplands. Next to the gently raising northeastern wall of Wide Ares Vallis, grooves  
976 degrade into transversal, relatively small ridges. Wing-shaped deposits overlie downstream portion of  
977 uplands and nearby grooved terrains. Wrinkle ridges (Wr) clearly postdate other features. Mosaic of HRSC  
978 h0155\_0001 and THEMIS V12795005, V04782003, V10349017, and V14330014 images. b) Three-  
979 dimensional view of streamlined uplands; mosaic of HRSC and THEMIS VIS images draped on HRSC  
980 DTM. c) Transversal and longitudinal topographic profile of streamlined uplands derived from HRSC DTM.  
981 d). Sketch illustrating a possible origin of streamlined uplands.

982

983 Fig. 11. Possible giant bar in an alcove sculpted along the right wall of the narrowest portion of Ares Vallis.  
984 Nadir a) and 3D view b) of a portion of HRSC h1022\_0000 image. c) Close-up: possible boundary between  
985 the giant bar and the grooved terrain is highlighted (MOC Na R0401710 ). d) Topographic profiles obtained  
986 from HRSC DTM.

987

988 Fig. 12. Pendant bars at the terminal reach of Ares Vallis; see fig. 9 for location. a) Parabolic erosional scour  
989 (S) forms upstream of the bedrock projection because of acceleration of flow in nearness of a bedrock  
990 projection; HRSC h2002\_0001 image. b) Three-dimensional view of Pb1; HRSC image draped on HRSC  
991 DTM. c) Sediments emplaced on the inner and deeper portion of troughs during the final stage of  
992 catastrophic floods overlap parabolic scours and lower portions of pendant bars; HRSC h1154\_0001 image.  
993 d) Three-dimensional view of Pb2; HRSC image draped on HRSC DTM. e) Close-up of a pendant bar:  
994 bedrock projection (Bp) and pendant bar (Pb3) are easily distinguishable. Laterally to the pendant bar, small  
995 troughs (solid lines) formed because of enhancement of flow energy: arrows indicate flow direction; wrinkle  
996 ridge (Wr) postdates the last depositional event. Portion of MOC E2200200 image. f) Interpretative sketch  
997 illustrating development of a pendant bar.

998

999 Fig. 13. a) HRSC mosaic of a cataract-like feature; see fig. 4 for location. Cataract-like feature (C) forms  
1000 next to a scarp (F) and successively extends upstream for about 35 kilometers by backward erosion of the  
1001 headwall. Grooved terrain (G), pendant bar (Pb) and streamlined upland (Su) occur upstream of the cataract-  
1002 like feature. Downstream of the cataract-like feature, all these erosional morphologies disappear; only a few  
1003 small streamlined remnants (R) occur. Notice sapping channels (S) emanating from a geological contact  
1004 between two different layers forming Noachian plateau, and hanging on Ares Vallis. HRSC h1022\_0000 and  
1005 h1011\_0000 image mosaic. b) Three-dimensional view of the area; HRSC mosaic draped on HRSC DTMs  
1006 mosaic; vertical exaggeration = 5.

1007

1008 Fig. 14. a) Several coalescing, flat-floored, depressions (Td), possibly thermokarstic in origin, characterize  
1009 materials infilling Eastern Valley Crater. Smaller and shallower depressions (sTd) appear not connected to  
1010 others. Eastern Valley incises and postdates the coalescing depressions. Mosaic of HRSC h0912\_0000 and  
1011 h0901\_0000 images; see fig. 1 for location. b) Sketch illustrating a possible geomorphological evolution of

1012 Eastern Valley Crater. Flooding and non-flooding periods alternate. During the flooding period ice-rich  
1013 deposits were emplaced, while during the non-flooding period ice wasted. The non-flooding period must  
1014 have been long enough to allow the shaping of thermokarstic depressions.

1015

1016 Fig. 15. a) A bifurcating ridge (Br) outcrops on the valley floor, and possibly represents an ice-walled stream  
1017 deposit evolved after ice wasting. Black arrows indicate flow directions of the inferred ice-walled stream. A  
1018 fault (F) truncates the upstream portion of Br. Polygonal terrains (Pt) outcrop at the bottom of closed  
1019 depressions (which often appear as exhumed impact crater) and postdate Br. Meandering channel (Mc)  
1020 emanating from the flat-floored impact crater (C) and thermokarstic depressions (Td) etches erosional  
1021 terraces (t1-t4); Ares Vallis truncates and postdates the meandering channel. HRSC h0945\_0000 e  
1022 h0934\_0000 images mosaic; see fig. 1 for location. b) Three-dimensional close-up. Br bifurcates next to a  
1023 streamlined hill (Sh): the up-convex northern branch of Br suggests that at least this portion of the ice-walled  
1024 stream flowed in a sub-ice tunnel. Erosional terraces shaped during later catastrophic flood events (t2-t4) are  
1025 poorly developed with respect to the first one (t1), and then are not easily distinguishable. Notice the  
1026 meandering channel Mc termination hanging on Ares Vallis. HRSC mosaic draped on HRSC DTMs mosaic.  
1027 Vertical exaggeration = 3.

1028

1029 Fig. 16. Close-ups and context image of probable kame features and underlying grooved terrains  
1030 characterizing Wide Ares Vallis. a) Topmost part of the largest probable kame features appears to be etched  
1031 by thermokarstic depressions (Td) of which floors streamlined features and patches of underlying grooved  
1032 terrains (dashed lines) commonly outcrop. b) Polygonal terrains (Pt) surround probable kame features  
1033 occurring at the inner and deeper portions of the valley. Arrows highlight the layered structures of probable  
1034 kame features. c) Probable kame features showing reticulated shape (dashed lines). d) Rising rim (Rr) on top  
1035 of a probable kame feature. Portion of MOC R1800149. e) Individual probable kame features show various  
1036 layering: a dark layer clearly occurs on the wall of the probable kame K1, while is not observable on the  
1037 neighboring probable kame K2. Portion of MOC M2001237. f) Context image for image a, b, c, and figure 7.  
1038 Image HRSC h1066\_0000.

1039

1040 Fig. 17. a) Interpretative three-dimensional sketch illustrating relationships among erosional terraces,  
1041 probable kame features, and the Ares Vallis floor. Sinuous channels partially etch the outermost grooved  
1042 terraces (t1) and run toward the inner portion of Ares Vallis. Toward downstream, channels turn into  
1043 elongated, slightly sinuous ridges and mesas (K), which overlie the innermost terraces (t1-2) and extend on  
1044 valley floor (Vf). THEMIS V12770013, V10012003, and V13394008 mosaic draped on HRSC h0155\_0001  
1045 stereo-derived DTM; vertical exaggeration = 3. b) Sketch illustrating a possible geological evolution of  
1046 probable kame features. 1) Subsequent to catastrophic flood processes Ares Vallis was infilled by ice; 2)  
1047 stream of water carved sinuous channels on both areas uncovered by ice and on the ice mass, emplacing  
1048 fluvio-glacial deposits; 3) Ice wasting caused the landscape inversion, originating sinuous ridges and mesas  
1049 consisting of fluvio-glacial deposits. The thickness and spatial distribution of such kame features imply that  
1050 an ice mass up to hundreds of meters thick infilled Ares Vallis at the time in which fluvio-glacial deposits  
1051 were emplaced.

1052

1053 Fig. 18. Pitted terrains consist of areas dotted by numerous hollows tens of meters wide. Such terrains show  
1054 higher radiance values in THEMIS IR nighttime image with respect to nearby areas (see the color-coded  
1055 bar). Association of such morphological and thermal properties suggests that ground-ice occurred in the past  
1056 (and possibly at the present day) and that pits originated by ground-ice wasting. a) In the terminal reach of  
1057 Aram Chaos Channel, pitted terrains occur exclusively at the valley floor (Vf), and they lack on valley walls  
1058 and terraces (T); data fusion of MOC E0301279 and THEMIS IR Night mosaic; see fig. 3 for location. b) On  
1059 the floor of Eastern Valley Crater, pitted terrains occur on top of crater floor deposits (Cf), and as patches at  
1060 the bottom of thermokarstic depressions (Td), where they are less distinguishable. Walls of thermokarstic  
1061 depressions show layering (at least four) tens of meters thick; arrows indicate boundaries (b1, b2, b3) among  
1062 different layers. Data fusion of MOC E1700126 and THEMIS IR Night mosaic; see fig. 14 for location.

1063

1064 Fig. 19. Three-dimensional view of a portion of the narrow reach of Ares Vallis. Here valley terrace  
1065 collapsed as a slump that overlaps and postdates grooved terrains (G) and valley floor. The slump deposit  
1066 shows a pitted patterned surface (P), suggesting burying of ice and the following activity of periglacial  
1067 processes. Notice the thermokarstic depressions (Td) etched on the terrace. HRSC h0934\_0000 and  
1068 h0923\_0000 images mosaic draped on HRSC DTMs mosaic; vertical exaggeration = 3.

1069

1070 Fig. 20. Sketch (not to scale) illustrating cyclic events responsible for sculpting of Ares Vallis. 1) An  
1071 enormous flood discharged from chaotic terrains and sculpted Ares Vallis. 2) It shaped grooved terrains and  
1072 other erosional morphologies at its base, while ice cover formed on its top because of Martian climatic  
1073 condition. Grooved terrains form by powerful vortices acting at the base of the flood. 3) During the waning  
1074 stage of flood, a relatively thin sheet of water flowed at the bottom of a thick ice-cover. In this condition,  
1075 sculpting of grooves was enhanced. 4) At the end of the flood the ice-cover grounded on the valley floor  
1076 forming a thick mass of dead-ice. Climate started to be warmer and wetter because of greenhouse effect of  
1077 water vapor and carbon dioxide/methane gas released during catastrophic floods. 5) Such climatic condition  
1078 favored ice melting and allowed presence of liquid water on the surface, which etched the ice mass forming  
1079 ice-walled channels and lakes, besides thermokarstic depressions. 6) Greenhouse effect faded and liquid  
1080 water disappeared from the surface. Climate progressively came back to cold-dry conditions. 7) In such  
1081 climatic condition ice continued to waste by the prevailing sublimation process. Materials deposited on the  
1082 floor of ice-walled channels and lakes became kame features, which overlie both grooved terrains and  
1083 streamlined features. The pristine appearance of grooved terrains and kame features suggests that colder-  
1084 dryer conditions prevailed during most part of ice-mass wasting. 8) Ice mass totally wasted and it caused the  
1085 ice-contact features to be overlying erosional features. If some catastrophic floods occurred during wet-warm  
1086 climatic conditions, they probably were ice-free. In this case floods simply deepened Ares Vallis, removing  
1087 ice masses and ice-related features occurring on the valley floor.

